BIOCHEMICAL PHARMACOLOGY 72 (2006) 1246–1256

available at www.sciencedirect.com

ScienceDirect

journal homepage: www.elsevier.com/locate/biochempharm

Inhibition of phosphatidylinositol 3-kinase-mediated glucose metabolism coincides with resveratrol-induced cell cycle arrest in human diffuse large B-cell lymphomas

Anthony C. Faber [a], *Fay J. Dufort* [a], *Derek Blair* [a], *Dean Wagner* [a], *Mary F. Roberts* [b], *Thomas C. Chiles* [a,*]

[a] *Department of Biology, Boston College, 414 Higgins Hall, Chestnut Hill, MA 02467, United States*
[b] *Department of Chemistry, Boston College, Chestnut Hill, MA 02467, United States*

ARTICLE INFO

Article history:
Received 7 June 2006
Accepted 8 August 2006

Keywords:
Resveratrol
Phosphatidylinositol 3-kinase
Cell cycle
Glycolysis
Diffuse large B cell lymphoma

ABSTRACT

An abnormally high rate of aerobic glycolysis is characteristic of many transformed cells. Here we report the polyphenolic compound, resveratrol, inhibited phosphatidylinositol 3-kinase (PI-3K) signaling and glucose metabolism, coinciding with cell-cycle arrest, in germinal center (GC)-like LY1 and LY18 human diffuse large B-cell lymphomas (DLBCLs). Specifically, resveratrol inhibited the phosphorylation of Akt, p70 S6K, and S6 ribosomal protein on activation residues. Biochemical analyses and nuclear magnetic resonance spectroscopy identified glycolysis as the primary glucose catabolic pathway in LY18 cells. Treatment with the glycolytic inhibitor 2-deoxy-D-glucose, resulted in accumulation of LY18 cells in G_0/G_1-phase, underscoring the biological significance of glycolysis in growth. Glycolytic flux was inhibited by the PI-3K inhibitor LY294002, suggesting a requirement for PI-3K activity in glucose catabolism. Importantly, resveratrol treatment resulted in inhibition of glycolysis. Decreased glycolytic flux corresponded to a parallel reduction in the expression of several mRNAs encoding rate-limiting glycolytic enzymes. These results are the first to identify as a mechanism underlying resveratrol-induced growth arrest, the inhibition of glucose catabolism by the glycolytic pathway. Taken together, these results raise the possibility that inhibition of signaling and metabolic pathways that control glycolysis might be effective in therapy of DLBCLs.

1. Introduction

Resveratrol exhibits anti-oxidant and anti-inflammatory activities. These biological activities have been linked to inhibition of cyclooxygenase and free radical formation [1–3]. Resveratrol suppresses signaling through the IκB kinase/NF-κB pathway, which is likely to contribute to its anti-inflammatory activity [4,5]. Jang et al. [3] reported the ability of resveratrol to block tumor initiation, promotion, and progression. Cell cycle arrest induced by resveratrol results, at least in part, from inhibition of enzyme activities directly involved in DNA synthesis and the up-regulation of p53 and p21 [6–9]. The pro-apoptotic effects of resveratrol have been linked to several mechanisms, including perturbation of mitochondrial permeability, caspase-9 activation, and CD95-signaling [10–14]. Despite these advances, much remains to be known of the mechanism(s) underlying the anti-proliferative action of resveratrol. Moreover, its efficacy in human diffuse large B-cell lymphomas (DLBCLs) has not been investigated.

* *Corresponding author*. Tel.: +1 617 552 0840; fax: +1 617 552 3130.
E-mail address: ChilesT@bc.edu (T.C. Chiles).
0006-2952/$ – see front matter
doi:10.1016/j.bcp.2006.08.009

Diffuse large B-cell lymphoma is the most common form of non-Hodgkin's lymphoma (NHL) [15–17]. A subset of patients with DLBCL can be successfully treated with conventional anthracycline-based chemotherapy [17]. The variability in response to chemotherapy along with the biologic heterogeneity suggests that DLBCL comprises several diseases [15,16]. Gene expression profiling studies have revealed DLBCL to be comprised of at least three distinct sub-groups, germinal center (GC)-like, activated B-cell (ABC)-like, and primary mediastinal PM-BCL [18–22]. ABC-DLBCLs exhibit constitutively active NF-κB, which is necessary for survival, whereas GC-DLBCLs express a ''signature'' gene profile reflecting that of normal tonsillar GC B cells [18,20,23]. GC-DLBCLs also express a glycolysis ''sub-signature'' gene profile; however, the biological significance of increased glycolytic gene expression has not been established [18]. Advances in the treatment of DLBCL will require the identification and functional analysis of the signaling molecules and metabolic pathways active in individual DLBCL sub-groups.

Phosphatidylinositol 3-kinase (PI-3K) contributes to the activation of growth and anti-apoptotic pathways [24]; aberrant expression and/or activation of PI-3K have been linked to several human diseases such as diabetes and malignancy [25,26]. PI-3Ks are classified as IA, IB, II, and III; the class I isoforms phosphorylate the D3 hydroxyl of phosphoinositides, thereby generating lipid mediators such as phosphatidylinositol 3,4,5-trisphosphate (PIP_3) [25,26]. PIP_3 recruits to the cell membrane proteins that contain pleckstrin-homology domains, such as protein kinase B (Akt) and this facilitates their activation [27]. Akt coordinates multiple cellular functions through phosphorylation-dependent activation of distinct signaling cascades [24,25,28–30]. The role of PI-3K/Akt signaling in the growth and/or survival of GC-DLBCLs has not been thoroughly investigated. Here we report that resveratrol treatment of the human LY1 and LY18 GC-DLBCLs results in G_0/G_1-phase cell cycle arrest and evidence is provided that growth arrest by resveratrol occurs through disruption of PI-3K signaling and inhibition of glucose catabolism via glycolysis.

2. Materials and methods

2.1. Antibodies and reagents

Anti-phospho-FOXO3a (S253) antibody (Ab) was purchased from Upstate Cell Signaling Solutions (Charlottesville, VA). The anti-phosho-p70 S6K (T389), anti-phospho-Akt (S473), anti-Akt, anti-phospho-JNK (T183/Y185), anti-phospho-p38MAPK (T180/Y183), anti-phospho-MEK1/2 (S217/S221), anti-phospho-S6 ribosomal protein (S235/S236), and anti-MEK1/2 antibodies (Abs) were obtained from Cell Signaling Technology (Beverly, MA). Anti-β-actin Abs and anti-hsp90 Abs were obtained from Stressgen Biotechnologies Corp. (Victoria, BC). ECL reagents were obtained from Kirkegaard and Perry Laboratories (Gaitherburg, MD). FITC-conjugated Annexin V and anti-CD16/CD32 (FcγIII/II receptor) 2.4G2κmAb were obtained from BD Biosciences (San Diego, CA). The anti-Glut1 Ab was from Fitzgerald Industries International (Concord, MA). PE-conjugated $F(ab')_2$ fragments of goat anti-rabbit IgG was obtained from CalTag Laboratories (Burlingame, CA). Resveratrol was obtained from Sigma–Aldrich (St. Louis, MO). All other reagents were purchased from Calbiochem-Novabiochem International (San Diego, CA).

2.2. Cell culture

Dr. Raju Chaganti (Memorial Sloan-Kettering Cancer Center, New York, NY) kindly provided the human GC-like DLBCL cell lines OCI-Ly1 (LY1) and OCI-Ly18 (LY18). The cells were maintained in a 37 °C-humidified incubator (5% CO_2) and cultured as previously described [31]. Cells were treated with the desired doses of resveratrol (25 or 50 μM final concentration in tissue culture medium) dissolved in dimethyl sulfoxide (DMSO) or DMSO alone as a control. The dose range of resveratrol used in this study is consistent with reports evaluating either the anti-inflammatory or anti-proliferative actions of resveratrol on numerous cell and tissue types (1–10).

2.3. Flow cytometry and cell cycle analysis

LY1 (5×10^5) or LY18 (5×10^5) cells were collected, washed in PBS, and then resuspended in PBS containing 0.1% Triton X-100, 50 μg/ml propidium iodide (PI) and 50 μg/ml RNase A. Cells were incubated for 30 min (37 °C) and DNA content was measured by flow cytometry using a FACSCanto cytometer (BD Biosciences). Acquired data were analyzed with Modfit LT V3.0 (Verity Software House, Tosham, ME). For apoptosis measurements, cells (5×10^5) were collected, washed in PBS and then resuspended in 0.5 ml binding buffer (10 mM HEPES, pH 7.4, 140 mM NaCl, 2.5 mM $CaCl_2$) containing 5 μl of FITC-conjugated Annexin V and 5 μl PI (50 μg/ml). Cells were incubated at room temperature for 15 min and then analyzed by flow cytometry. Staining of surface Glut1 expression was carried out as previously described [32].

2.4. Western blotting

Cells were solubilized in Triton X-100 buffer (20 mM Tris, pH 7.4, 100 mM NaCl, 0.1% Triton X-100) containing 2.5 μg/ml leupeptin/aprotinin, 10 mM β-glycerophosphate, 1 mM PMSF, 1 mM NaF, and 1 mM Na_3VO_4. Insoluble debris was removed by centrifugation at 15,000 × *g* for 15 min (4 °C). Lysate protein was separated by electrophoresis through a 10% polyacrylamide SDS gel, transferred to an Immobilon-P membrane, and incubated with the indicated Abs as described [32].

2.5. Glucose utilization

Glucose transport was measured by monitoring the uptake of 100 μM 2-deoxy-D-glucose plus 1 μCi/ml [^{3}H]2-deoxy-D-glucose (Amersham Biosciences, Piscataway, NJ) as previously described [32,33]. To assess the contribution of total glucose uptake by facilitated glucose transporters, uptake of [^{3}H]2-deoxy-D-glucose was also measured in the presence of 10 μM cytochalasin B, a potent inhibitor of glucose transporter activity. Glycolysis was measured by incubating 10^6 LY18 cells/0.5 ml with 2 μCi [5-^{3}H]glucose (Amersham Biosciences) for 90 min. Cells (100 μl) were removed and placed in 1.5 ml microcentrifuge tubes containing 100 μl of 0.2N HCl ^3H_2O was

separated from unmetabolized [^{3}H]glucose by evaporation diffusion for 48 h (25 °C) as previously described [32,33]. Oxidation of glucose was measured by monitoring the rate of $^{14}CO_2$ production from LY18 cells cultured with 1 μCi [6-^{14}C]glucose (Amersham Biosciences) as described [32]. Glucose and lactate levels were measured using assay kits from Sigma Diagnostics (St. Louis, MO) according to the manufacturer's instructions.

2.6. Real-time RT-PCR

Total RNA was isolated from LY18 cells using the RNeasy mini RNA isolation kit (QIAGEN Inc., Valencia, CA), following the manufacturer's protocol. Following DNase-I treatment, 2 μg RNA was reverse-transcribed to cDNA using MMLV reverse transcriptase (Ambion Inc., Austin, TX). Real-time PCR was performed with the SYBR Green Supermix on an iCycler with iQ5 Real-time PCR detection system (Bio-Rad Laboratories, Hercules, CA). Amplification conditions were as follows: 50 °C for 2 min, 95 °C for 10 min, followed by 45 cycles of 95 °C for 15 s, 58 °C for 1 min. Real-time primers contained a specified amplicon length of between 150 and 200 bp. Primers were as follows: β2 microglobulin, forward: 5′-AGGAGACACGGAACAC-CAAGG-3′, reverse: 5′-CCATCGTAGGCATACTGTTCATACC-3′; hexokinase-2, forward: 5′-ACGAGAGCATCCTCCTCAAGTG-3′, reverse: 5′-GGTCTTCAAAGCCACAGGTCATC-3′; phosphoglycerate mutase-1, forward: 5′-GGACAGTGCTAGATGCCATTGATC-3′, reverse: 5′-CGGAGGTGGTGG GACATCATAG-3′; and phosphofructokinase-1, forward: 5′-GGCAACCTGAACACCTACAA-GC-3′, reverse: 5′-CGAAGCCGTCAAAGCCATCA TAG-3′. Relative expression of RNA was determined as the relative expression = $2^{-(\Delta\Delta CT)}$, where ΔΔCT = (cycle threshold (CT) gene of interest) − (CT β2 microglobulin). Real-time SYBR-green dissociation curves show one species of amplicon for each primer combination (data not shown).

2.7. Nuclear magnetic resonance (NMR) spectroscopy

LY18 cells (3×10^7) were cultured in RPMI 1640 containing 10 mM [1-^{13}C]glucose or [2-^{13}C]glucose (Cambridge Isotope Laboratories Inc., Andover, MA). Cells were collected by centrifugation and extracted three times with 1 ml of 70% (v/v) ethanol. The soluble ethanol extracts were pooled, frozen in liquid nitrogen and lyophilized. The dry material was then resuspended in 0.5 ml D_2O. ^{1}H and ^{13}C-coupled ^{1}H spectra were acquired on a Varian INOVA 500 spectrometer (Varian Inc., Palo Alto, CA) with a 5 mm indirect detection probe as described previously [32,34]. ^{1}H NMR spectra were acquired using a 5006.6 Hz sweep width, 9984 datum points, 90° pulse width, 3.0 s recycle delay time and 128 transients. The 1D heteronuclear multiple quantum coherence (HMQC) spectra (which detect only those protons coupled to ^{13}C) were acquired with a sweep width of 7509.6 Hz, 2048 datum points, 90° pulse width, a 1.0 s recycle delay time; these 1D spectra were also ^{13}C decoupled using 135 Hz as the average one-bond ^{1}H–^{13}C *J*-coupling constant. 1D HMQC spectra were obtained with 4000 transients. Under these acquisition conditions, the lactate methyl doublet was not resolved, but integrated intensities of small molecules could easily be quantified.

3. Results

3.1. Resveratrol inhibits growth of human LY1 and LY18 cells

To investigate the effects of resveratrol on growth, LY1 and LY18 cells were cultured in the presence or absence of resveratrol and the number of viable cells was measured over the course of 72 h. As shown in Fig. 1A, resveratrol caused a complete block of cell proliferation. Analysis of DNA content by PI staining and flow cytometry indicated that in the presence of 25 or 50 μM resveratrol, LY1 and LY18 cells accumulated in G_0/G_1-phase of the cell cycle when measured at 24 h (Fig. 1B). Resveratrol-treated cultures also exhibited increased hypodiploid DNA content in comparison to control non-treated LY1 or LY18 cells at 24 h, signifying apoptotic cells (Fig. 1B). The presence of apoptotic cells was confirmed by annexin V-FITC staining. Although control LY1 and LY18 cells exhibited measurable annexin V-FITC positive cells, treatment with 25 or 50 μM resveratrol for 24 h led to an increase in the percentage of apoptotic cells (Fig. 1C).

3.2. LY1 and LY18 cells display PI-3K signaling that is inhibited by resveratrol

To understand the mechanism(s) underlying resveratrol-induced growth arrest, we examined the effects of resveratrol on several pathways known to control growth in naïve B lymphocytes [24,25]. LY18 and LY1 cells displayed phosphorylated Akt on Ser473, which is necessary for full activation of the kinase (Fig. 2A and B, respectively). The downstream target of Akt, p70 S6K exhibited phosphorylation on Thr389, which is required for activation. In addition, S6 ribosomal protein and FOXO3a were phosphorylated on residues Ser235/236 and Ser253 in LY18 and LY1 cells, respectively (Fig. 2A and B); members of the FOXO family of transcription factors are targets of Akt [28]. The contribution of PI-3K to the phosphorylation of these signaling components in LY18 cells was demonstrated insofar as treatment with the PI-3K inhibitor LY294002, reduced phosphorylation of Akt, p70 S6K, S6 ribosomal protein, and FOXO3a (Fig. 2C). Treatment of LY18 cells with rapamycin, an inhibitor of mTOR, blocked p70 S6K and S6 ribosomal protein phosphorylation, confirming the role of mTOR as an upstream effector of these components (Fig. 2E). Similar results were obtained following LY294002 or rapamycin treatment of LY1 cells (Fig. 2B, D and F).

Treatment of LY1 or LY18 cells for 4 h with 25 or 50 μM resveratrol inhibited downstream PI-3K signaling, as evidenced by reduced phosphorylation of Akt, p70 S6K, S6 ribosomal protein and FOXO3a on the aforementioned residues (Fig. 2A and B). The effects of resveratrol cannot be attributed to a global inhibition of signaling, because the phosphorylation of JNK (Thr183/Tyr185) and p38 MAPK(Thr180/Tyr182) was not inhibited by resveratrol treatment of LY18 (Fig. 3A) or LY1 cells (data not shown). Importantly, we find that PI-3K signaling was required for cell cycle progression insofar as treatment of LY1 or LY18 cells with LY294002 blocked proliferation (Fig. 3B) and that this was accompanied by an increased percentage of cells in G_0/G_1-phase of the cell cycle in comparison to control non-treated

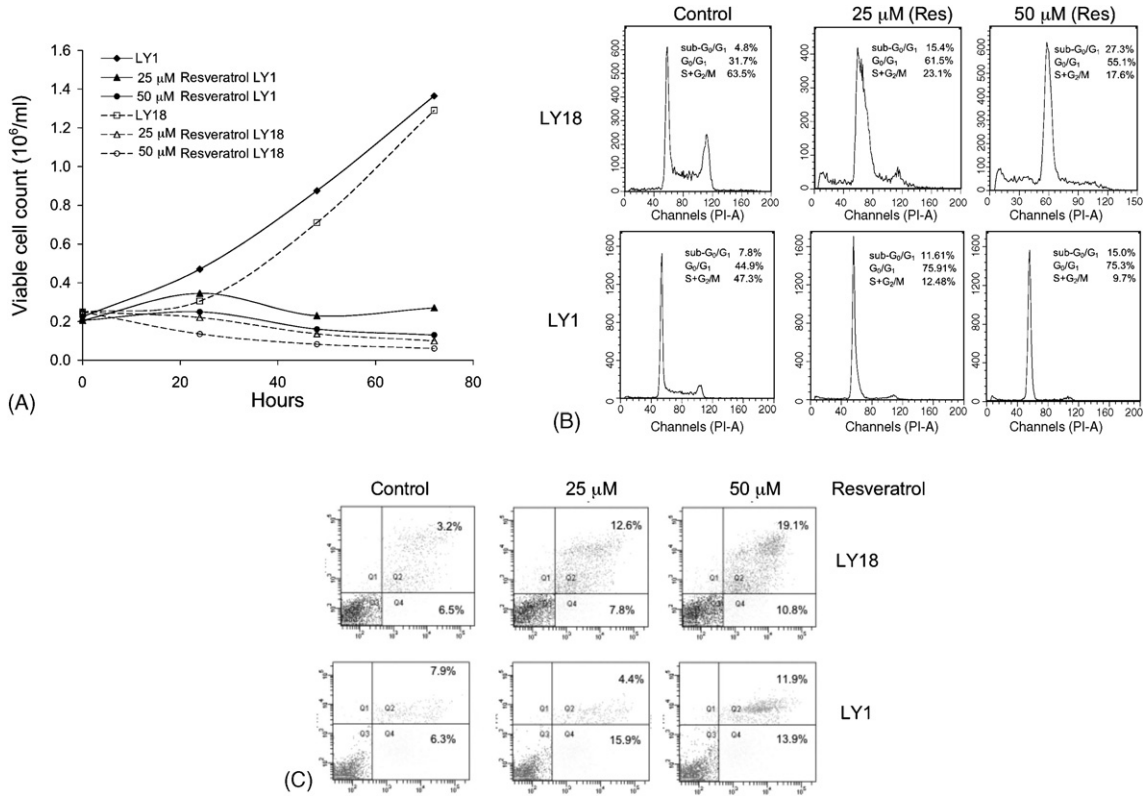

Fig. 1 – Resveratrol inhibits human LY1 and LY18 cell growth. (A) LY1 and LY18 cells were cultured in medium containing DMSO (as solvent control, denoted hereafter as Control) or in the presence of 25 or 50 μM resveratrol (Res). At the indicated times, the number of viable cells was determined by trypan blue exclusion; similar results were obtained with PI staining/flow cytometry (data not shown). The data are representative of three independent experiments; the standard deviation is less than 5% of the mean (not indicated on the graph). (B) Cells were cultured in the absence (Control) or presence of 25 or 50 μM resveratrol for 24 h and then analyzed for DNA content by PI staining/flow cytometry as described in Section 2. (C) LY1 and LY18 cells were also cultured in the absence (Control) or presence of 25 or 50 μM resveratrol for 24 h and the percentage of apoptotic cells was determined by Annexin V and PI staining as described in Section 2. For (B and C), the data are representative of four independent experiments.

LY18 (Fig. 3C) or LY1 cells (data not shown). Consistent with these results, treatment with triciribine, a cell-permeable tricyclic nucleoside that specifically inhibits Ser473 phosphorylation (Fig. 3C, inset) and activation of Akt [35], resulted in an increase in the percentage of LY18 cells in G_0/G_1-phase of the cell cycle at 24 h (Fig. 3C); rapamycin similarly induced the accumulation of LY18 cells in G_0/G_1-phase of the cell cycle (Fig. 3C). Taken together with the anti-proliferative action of resveratrol (Fig. 1), these findings suggest that resveratrol blocks LY1 and LY18 cell growth, in part, by inhibiting PI-3K signaling.

During the course of these studies, we observed that MEK1/2 was phosphorylated on activation residues Ser217/221 in LY18 (Fig. 3A) and LY1 cells (data not shown). Moreover, resveratrol reduced MEK1/2 phosphorylation, as shown in the LY18 DLBCL (Fig. 3A). In keeping with the established role of MEK1/2 in mammalian cell proliferation, these results point to a role for MEK1/2 in resveratrol-induced growth arrest. However, treatment of LY1 or LY18 cells with several MEK1/2 inhibitors, including PD98059, U0126, or 2-chloro-3-(N-succinimidyl)-1,4-naphthoquinone (MEK II inhibitor), had no measurable effect on cell cycle distribution (Fig. 3D).

3.3. *Resveratrol inhibits PI-3K-linked glycolysis in LY18 cells*

Gene expression profiling has uncovered increased expression of several mRNAs encoding glycolytic enzymes in GC-DLBCLs, but not ABC-DLBCLs, raising the possibility that heightened glycolysis plays a role in the growth and/or survival of GC-DLBCLs [18,37]. Therefore, we investigated glucose metabolism and whether resveratrol might act to inhibit glucose utilization in GC-DLBCLs. For these studies, we initially focused on LY18 cells and examined the effects of resveratrol on glucose uptake and metabolism. Exponentially growing LY18 cells exhibited facilitated glucose uptake, which was not significantly inhibited by treatment with resveratrol or LY294002 (Fig. 4A). We next determined if resveratrol altered the surface expression of Glut carriers [36]. LY18 cells express Glut1 (Fig. 4B), which represents the primary facilitated glucose transporter expressed on hematopoietic cells [32,33]. Treatment with resveratrol or LY294002 did not measurably alter the expression of Glut1 (Fig. 4B).

During these experiments we observed lactate accumulation in the tissue culture medium (Fig. 4C). The ratio of lactate

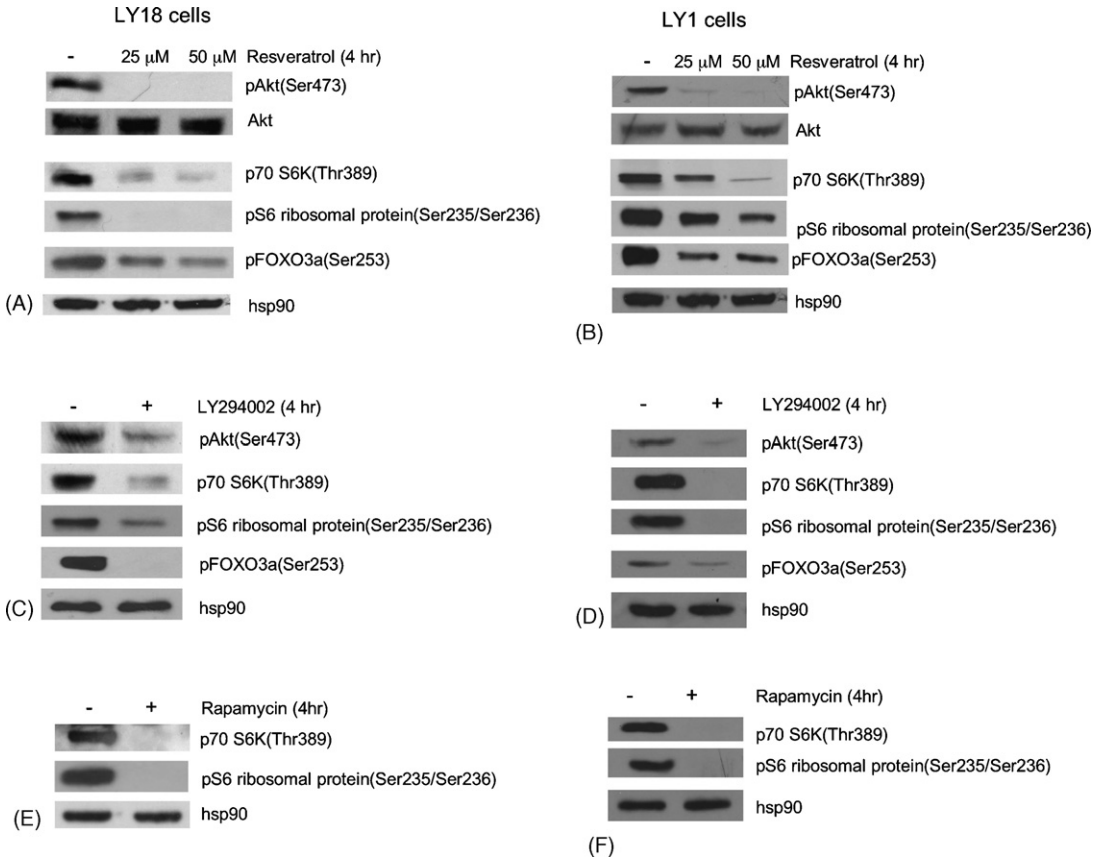

Fig. 2 – Resveratrol inhibits PI-3K signaling in LY1 and LY18 cells. Cells were cultured in the absence ((-) DMSO as solvent control) or presence of 25 or 50 μM resveratrol (A and B), 10 μM LY294002 (C and D), or 10 nM rapamycin (E and F) for 4 h. Cells were harvested and the phosphorylation of individual PI-3K signaling proteins was determined by Western blot analysis of detergent soluble whole cell extracts prepared from LY18 (A, C and E) and LY1 (B, D and F) cells. To control for protein loading, the blots were stripped and reprobed with anti-hsp90 Ab. The data are representative of four independent experiments.

produced/glucose consumed corresponded to approximately 1.8 at each time point, which was calculated from the cumulative glucose consumption from the tissue culture medium (0.9 and 2.0 mmol glucose at 12 and 24 h, respectively) and lactate production (1.6 and 3.6 mmol lactate, respectively) (Fig. 4C, lanes Control). If direct conversion of glucose to lactate is assumed, these data suggest that a significant portion of glucose consumed by LY18 cells is metabolized to lactate. Interestingly, the increase in lactate production over time was reduced by resveratrol treatment and was inhibited by LY294002 (Fig. 4C). To identify the glucose catabolic pathways functioning in LY18 cells, we evaluated glucose flux through glycolysis. LY18 cells exhibited a relatively high rate of glycolysis (Fig. 5A); treatment with resveratrol resulted in a greater than 70% reduction in glycolysis (Fig. 5A). Glycolysis was dependent on PI-3K activity as evidenced by reduction of glycolytic flux with LY294002, to a level comparable to that of resveratrol.

To corroborate the finding that resveratrol inhibits glycolysis, we used NMR spectroscopy to specifically monitor ^{13}C fixation from [1-^{13}C]glucose into metabolites. We have previously shown that the use of a 1D-HMQC sequence to select out protons attached to ^{13}C of [1-^{13}C]glucose and its metabolites afford measurement of glucose metabolism by the glycolytic pathway [32]. Integration of the ^{13}C-coupled ^{1}H resonances revealed that the lactate methyl group exhibited a relatively high ^{13}C content as [1-^{13}C]glucose was metabolized in LY18 cells (Fig. 5B, 1-^{13}C control, hatched bars). Resveratrol treatment of LY18 cells inhibited approximately 65% of ^{13}C label incorporation from [1-^{13}C]glucose into the methyl group of lactate (Fig. 5B, 1-^{13}C resveratrol, hatched bars). Similar results were obtained with LY18 cells treated with LY294002, although inhibition of PI-3K activity resulted in approximately 80% inhibition of ^{13}C label incorporation into the methyl group of lactate (Fig. 5B, 1-^{13}C LY294002, hatched bars).

To monitor for diversion of glucose into the pentose phosphate pathway, a similar 1D-HMQC experiment was carried out with [2-^{13}C]glucose. If [2-^{13}C]glucose is used instead of [1-^{13}C]glucose, we have previously shown that no ^{13}C label is incorporated into the lactate methyl group by the glycolytic pathway; however, if the pentose phosphate pathway is operational ^{13}C label will be incorporated into the methyl group of lactate [32]. A relatively small amount of ^{13}C label from [2-^{13}C]glucose was incorporated into the lactate methyl group when measured at 12 h (Fig. 5B, 2-^{13}C control, hatched bars). Treatment with resveratrol did not measurably reduce ^{13}C label

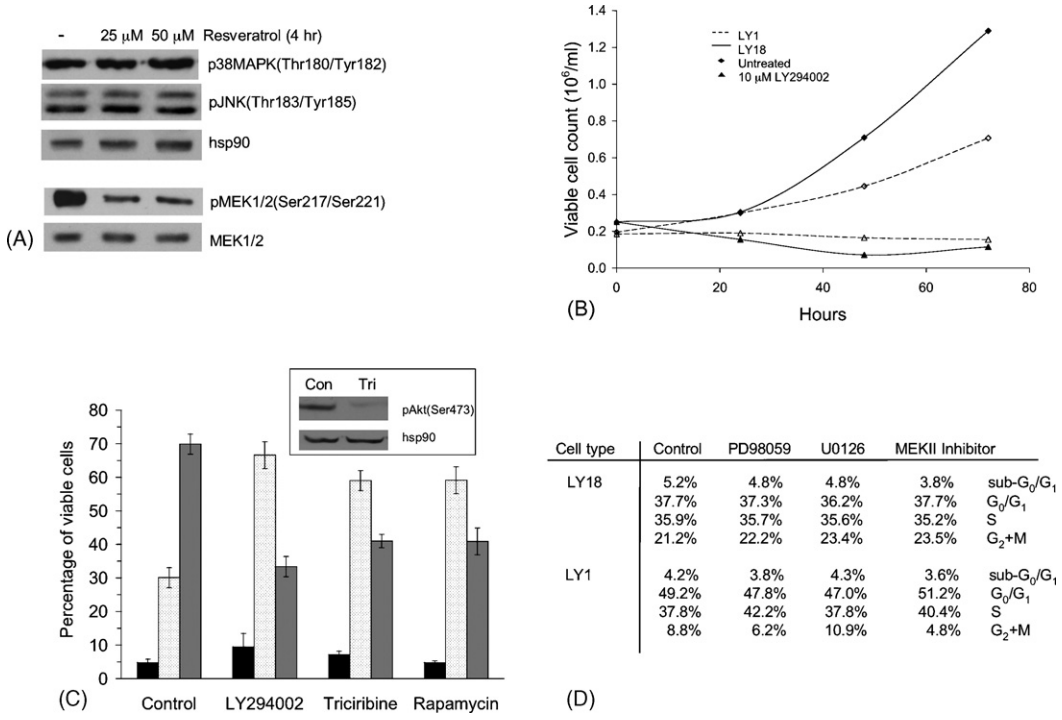

Cell type	Control	PD98059	U0126	MEKII Inhibitor	
LY18	5.2%	4.8%	4.8%	3.8%	sub-G_0/G_1
	37.7%	37.3%	36.2%	37.7%	G_0/G_1
	35.9%	35.7%	35.6%	35.2%	S
	21.2%	22.2%	23.4%	23.5%	G_2+M
LY1	4.2%	3.8%	4.3%	3.6%	sub-G_0/G_1
	49.2%	47.8%	47.0%	51.2%	G_0/G_1
	37.8%	42.2%	37.8%	40.4%	S
	8.8%	6.2%	10.9%	4.8%	G_2+M

Fig. 3 – Inhibition of PI-3K, but not MEK1/2 blocks LY1 and LY18 cell growth. (A) LY18 cells were incubated in the absence ((-) DMSO control) or presence of 25 or 50 μM resveratrol for 4 h. Cells were harvested and phosphorylation of JNK and p38 MAPK on activation residues was measured by Western blot analysis using anti-phospho-JNK or anti-phospho-p38MAPK Abs. The blot was stripped and reprobed with an anti-hsp90 Ab to control for loading. Cell extracts were also probed with an anti-phospho-MEK1/2 Ab. The blot was stripped and reprobed with anti-MEK1/2 Ab. (B) LY1 and LY18 cells were incubated in the absence (Untreated) or presence of 10 μM LY294002. At the indicated times, the number of viable cells was determined by trypan blue exclusion. The data are representative of three independent experiments; the standard deviation is less than 5% of the mean (not indicated on the graph). (C) LY18 cells were cultured in the absence (Control) or presence of 10 μM LY294002, 1 μM Triciribine, or 10 nM rapamycin for 24 h. Cells were then analyzed for DNA content by flow cytometry as described in Section 2 (bar code: black = percentage of sub-G_0/G_1, opened dots = percentage of G_0/G_1, gray = percentage of S + G_2/M). Inset shows LY18 cells cultured in the absence (Con) or presence of 1 μM Triciribine (Tri) for 15 min; cells were then harvested and phosphorylation of Akt on Ser 473 was measured by Western blot analysis using an anti-phospho(S473) Akt Ab. The blot was stripped and reprobed with an anti-hsp90 Ab to control for protein loading. (D) LY1 and LY18 were cultured in the absence (Control) or presence of 10 μM PD98059, 10 μM U0126, or 10 μM MEK II inhibitor for 24 h. Cells were collected and stained with PI and analyzed for DNA content by flow cytometry as described in Section 2. The data in (A)–(D) are representative of three independent experiments.

incorporation, whereas LY294002 decreased ^{13}C label incorporation into the lactate methyl group by approximately 50% (Fig. 5B, 2-^{13}C hatched bars). We also measured glucose flux through the tricarboxylate acid (TCA) cycle by monitoring the rate of $^{14}CO_2$ generation from the metabolism of radiolabeled [6-^{14}C]glucose. The complete oxidation of glucose was not substantial in comparison to its flux via the glycolytic pathway (Table 1). The rate of glucose oxidation, albeit low, was not measurably altered by treatment of LY18 cells with resveratrol or LY294002 (Table 1). Taken together, these findings suggest that glucose is primarily metabolized by glycolysis and that resveratrol acts to inhibit glycolytic flux in LY18 cells.

Table 1 – The catabolism of glucose in LY18 cells

	Control (nmol/10^6 cells/h)	50 μM resveratrol (nmol/10^6 cells/h)	10 μM LY294002 (nmol/10^6 cells/h)
Glycolysis	2175 ± 150	550 ± 30.0	600 ± 40.0
TCA cycle	0.10 ± 0.01	0.11 ± 0.01	0.10 ± 0.01

The rates of metabolic flux of radiolabeled glucose via glycolysis and TCA cycle in LY18 cells cultured in the absence (Control) or presence of 50 μM resveratrol or 10 μM LY294002 were determined at 12 h. The data in nmol/10^6 cells/h are represented as mean values of three determinations.

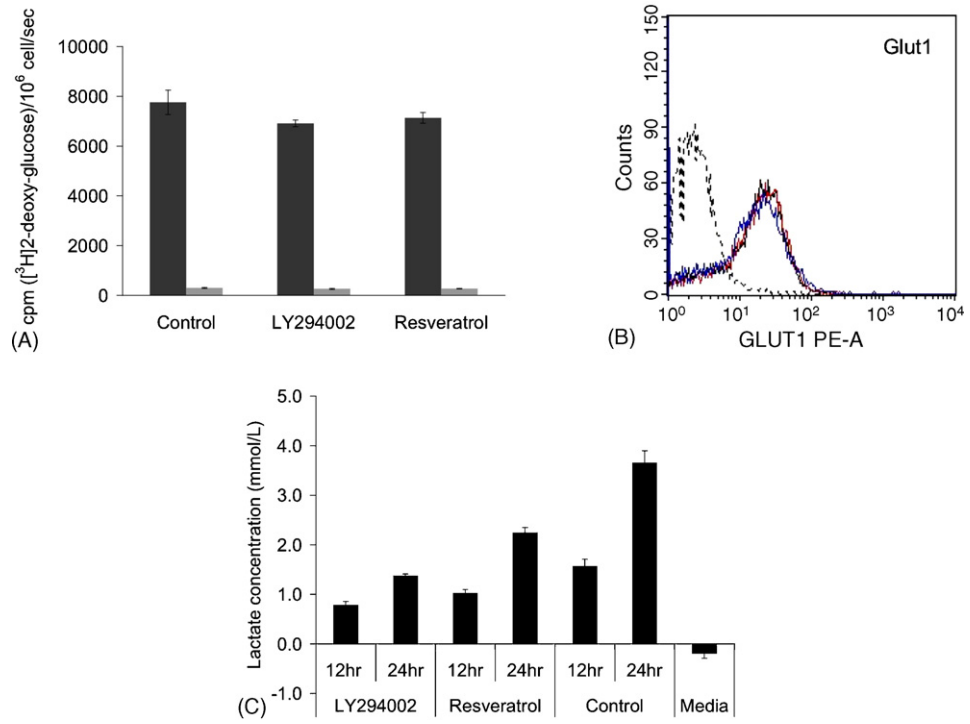

Fig. 4 – Facilitated glucose transport and Glut expression in LY18 cells. (A) LY 18 cells were cultured in the absence (Control) or presence of 50 μM resveratrol or 10 μM LY294002 for 12 h. Cells were harvested and uptake of [^{3}H]2-deoxy-D-glucose was measured for 60 s in the absence (black bars) or presence (gray bars) of 10 μM cytochalasin B. Error bars reflect standard deviation from the mean of triplicate measurements and the data are representative of two independent experiments. (B) LY18 cells were cultured in the absence (black line) or presence of 50 μM resveratrol (blue line) or 10 μM LY294002 (red line) for 12 h and then Glut1 expression was determined by flow cytometry as described in Section 2; the black dashed line indicates staining with an isotype control Ab. The data are representative of two independent experiments. (C) LY18 cells were cultured in the absence (Control) or in the presence of 10 μM LY294002 or 50 μM resveratrol. At the indicated times, the tissue culture medium was assayed for lactate levels (mmol/l) as described in Section 2. Media denotes the amount of lactate in tissue culture medium at the beginning of the experiment. Error bars reflect standard deviation from the mean of triplicate measurements and the data are representative of two independent experiments.

3.4. *Inhibition of glycolysis results in accumulation of LY18 cells in G_0/G_1-phase of the cell cycle*

The results above indicate that the anti-proliferative action of resveratrol may involve inhibition of glucose catabolism via the glycolytic pathway. To evaluate the contribution of glycolysis on cell cycle position, we treated LY18 cells with 2-deoxy-D-glucose (2-DOG) for 12 h and then analyzed cells by PI staining and flow cytometry. 2-DOG can be phosphorylated by hexokinase, but cannot be further metabolized through glycolysis [38]. As shown in Fig. 5C, inhibition of glycolysis resulted in accumulation of LY18 cells in G_0/G_1-phase of the cell cycle in comparison to control non-treated cells.

3.5. *Resveratrol reduced the expression of genes encoding rate-limiting glycolytic enzymes*

To obtain insight into the molecular basis underlying the inhibition of glycolysis by resveratrol, we evaluated the expression of several genes encoding enzymes in the glycolytic pathway. Treatment of LY18 cells with resveratrol resulted in decreased mRNA levels for hexokinase-2 and phosphofructokinase-1 by approximately 65% and 85%, respectively, relative to control non-treated LY18 cells (Fig. 5D). Both hexokinase-2 and phosphofructokinase-1 are rate-limiting enzymes for glycolysis. Interestingly, the expression of phosphoglycerate mutase-1 mRNA was decreased by approximately 75%. Our results also indicate that inhibition of PI-3K activity with LY294002 reduced mRNA expression for hexokinase-2 and phosphoglycerate mutase-1, which was similar to that observed with resveratrol (Fig. 5D). LY294002 reduced phosphofructokinase-1 mRNA levels by 50% (Fig. 5D).

4. Discussion

The results herein demonstrate that resveratrol treatment results in the accumulation of human LY1 and LY18 cells in G_0/G_1-phase of the cell cycle and that this is accompanied by inhibition of cell growth. Both lymphomas treated with resveratrol also exhibit an increase in annexin V staining and hypodiploid content of DNA, signifying apoptosis. Our studies show that LY18 and LY1 (data not shown) cells display activation of p38 MAPK and JNK, but resveratrol does not

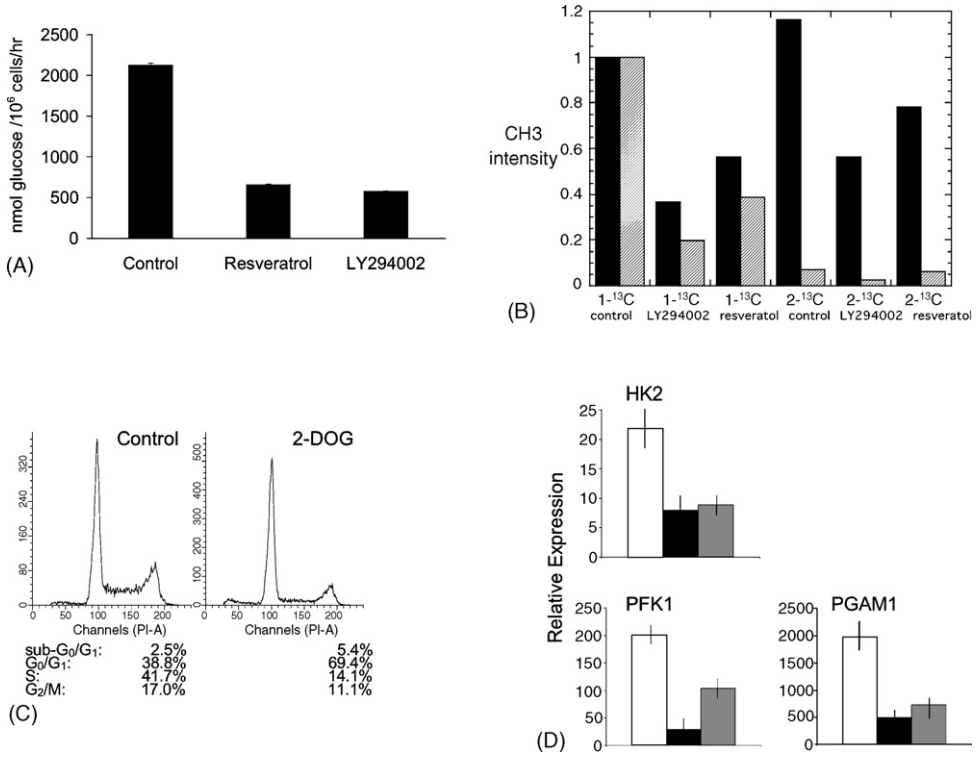

Fig. 5 – Resveratrol inhibits glycolysis in LY18 cells. (A) LY18 cells were cultured in the absence (Control) or presence of 10 μM LY294002 or 50 μM resveratrol (12 h) and then glycolysis was measured as described in Section 2. The standard error represents the mean of triplicate measurements and the data are representative of three independent experiments. (B) LY18 cells were cultured in medium alone (Control) or 10 μM LY294002 or 50 μM resveratrol for 12 h. The tissue culture medium was supplemented with 10 mM [1-^{13}C]glucose (1-^{13}C) or 10 mM [2-^{13}C]glucose (2-^{13}C) as indicated. Black bars indicate total lactate detected in the ^{1}H NMR spectrum; all values were normalized to the intensity of the control cells. Hatched bars indicate intensity of ^{13}C-coupled lactate methyl protons as measured using a 1D-HMQC NMR experiment described in Section 2; all intensities were normalized to the control sample ^{13}C-coupled proton intensity. (C) LY18 cells were cultured in the absence (Control) or presence of 10 mM 2-DOG for 12 h. Cells were collected and analyzed for DNA content by PI staining/flow cytometry as described in Section 2. (D) LY18 cells were cultured in medium alone (open bars), 50 μM resveratrol (black bars) or 10 μM LY294002 (gray bars) for 12 h. Cells were collected and Real-time RT-PCR was carried out as described in Section 2. Gene expression was evaluated for hexokinase-2 (HK2), phosphofructokinase-1 (PFK1), and phosphoglycerate mutase-1 (PGAM1). The data are presented as the standard deviation of the mean, $n = 3$. The experiment shown is representative of three independent experiments.

measurably affect the phosphorylation of these MAPKs on activation residues. These results are somewhat surprising given reports that MAPKs have been implicated in resveratrol-induced growth arrest and/or apoptosis of numerous cancer cell types [8,9,39]. By contrast, we found that LY18 and LY1 (data not shown) cells exhibit phosphorylation of MEK1/2. Interestingly, resveratrol treatment reduces MEK1/2 phosphorylation on activation residues; however, inhibition of MEK1/2 activity did not alter the cell cycle distribution of either human lymphoma. Although we cannot rule out a role for MEK1/2 in the cell cycle, these findings suggest that inhibition of MEK1/2 is not sufficient to induce growth arrest or apoptosis in LY1 or LY18 cells.

The experiments herein reveal that both LY1 and LY18 cells display continuous activation of the PI-3K pathway and that resveratrol inhibits PI-3K-dependent signaling. Our results suggest that PI-3K activity plays a role in cell cycle progression in that treatment with LY294002 blocks LY1 and LY18 cell growth. It should be mentioned that LY294002 is a potent PI-3K inhibitor, but has also been shown to inhibit other signaling molecules (reviewed in Ref. [25]). While this may represent a potential caveat to our interpretations of the role of PI-3K signaling in LY1 and LY18 cells, we note similar results with the PI-3K inhibitor wortmannin (data not shown). Moreover, in LY18 cells a similar inhibitory effect on the cell cycle was obtained in response to Akt or mTOR inhibition. Our results are consistent with a growing body of evidence that points to a role for PI-3K signaling in contributing to lymphomagenesis in leukemia and lymphoma [40,41].

The molecular basis underlying the activation of PI-3K signaling in LY1 and LY18 cells is unknown. The gene encoding the p110 subunit of PI-3K is highly expressed in GC-like DLBCL when compared to ABC-like tumors, suggesting that aberrant expression of the catalytic p110 subunit might contribute to the activation of PI-3K and downstream effectors of PI-3K signaling [18,37]. In addition, the tumor suppressor PTEN gene

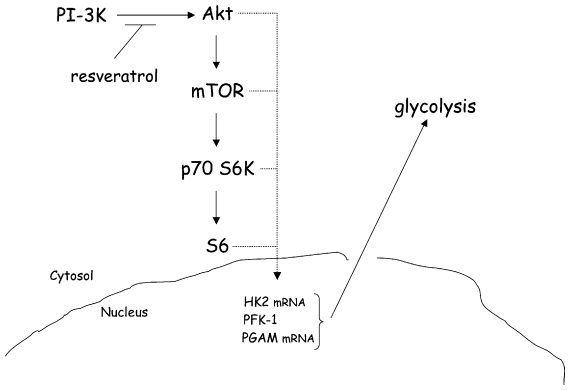

Fig. 6 – Model for the action of resveratrol in LY18 cells. Resveratrol inhibits downstream PI-3K signaling (Akt/mTOR/p70 S6K/S6) in LY18 cells. Although not entirely defined, components of this cascade lead to the transcriptional upregulation of several genes encoding enzymes in the glycolytic pathway, such as hexokinase II (HK2), phosphofructokinase-1 (PFK-1) and phosphoglycerate mutase-1 (PGAM) (denoted by dotted line). Expression of these gene products promote cellular glucose metabolism via glycolysis.

product, which antagonizes PI-3K signaling through its PtdIns(3,4,5)P_3 lipid phosphatase activity [42], is involved in 10q23 deletions in several tumors [43,44] and in approximately 5–10% of non-Hodgkin's lymphomas (reviewed in Ref. [16]). However, a recent study of NHL cases with 10q abnormalities did not display detectable biallelic deletions or mutations of PTEN [44]. Whether LY1 and LY18 cells contain deletions, mutations or exhibit haploinsufficiency of PTEN that might contribute to activation of PI-3K signaling remains to be investigated. Notwithstanding, our findings suggest that the anti-proliferative action of resveratrol on LY1 and LY18 DLBCLs results, at least in part, from inhibition of PI-3K signaling.

Our results indicate that glucose is primarily metabolized by the glycolytic pathway in LY18 cells. Similar results were obtained for LY1 cells (data not shown). We did not detect substantial oxidation of glucose by the TCA cycle. Because the assay used herein to monitor $^{14}CO_2$ generation requires the complete oxidation of [6-^{14}C]glucose, we cannot entirely rule out the possibility that some glucose may be incompletely oxidized by a "truncated" TCA cycle. The 1D-HMQC experiments reveal measurable glucose flux through the pentose phosphate pathway; however, in comparison to glycolytic flux, it was not substantial. These results are consistent with the elevated expression of several mRNAs encoding glycolytic enzymes detected by gene profiling of GC-DLBCLs [18,37]. We also provide data underscoring the importance of glycolysis in LY18 cell growth in that 2-DOG, which can be phosphorylated by hexokinase, but cannot be further metabolized through glycolysis [38], is sufficient to induce G_0/G_1-phase arrest in LY18 cells. It is noteworthy that many tumor cells exhibit high rates of aerobic glycolysis, regardless of whether oxygen is present to carry out oxidative phosphorylation in the mitochondria [45]. The so-called Warburg effect has been attributed to mutations in the mitochondrial respiratory chain or in glycolytic enzymes [46]; however a recent report indicates that activation of Akt alone is sufficient to account for the switch to glycolysis in tumor cells [29].

Importantly, our studies reveal for the first time that resveratrol inhibits glycolysis, which is accompanied by a reduction in lactate production (Fig. 6). The signaling pathway underlying resveratrol-induced effects on glycolytic flux in LY18 cells has not been completely defined. However, LY294002 similarly reduces glycolysis in exponentially growing LY18 cells, raising the possibility that resveratrol may inhibit glycolysis through its inhibitory action on PI-3K signaling. It is unlikely that decreased glycolytic flux is secondary to a reduction in glucose uptake, given that facilitated glucose uptake is not affected by resveratrol. Resveratrol treatment does however, result in a decrease in mRNAs encoding hexokinase-2 and phosphofructokinase-1, both are considered rate-limiting glycolytic enzymes. Interestingly, resveratrol also reduces phosphoglycerate mutase-1 mRNA, which encodes an enzyme of the glycolytic pathway that catalyzes the isomerization of 3- and 2-phosphoglycerates. Although this step is not considered to be rate-limiting in the majority of differentiated cell types, phosphoglycerate mutase-1 may be rate-limiting for glycolysis in tumor cells [47].

In conclusion, the results indicate that PI-3K signaling is an important mechanism for cell growth in LY1 and LY18 cells. Our results support the conclusion that PI-3K signaling is a pivotal target of resveratrol in LY1 and LY18 cells with an inhibitory effect on glucose metabolism that is necessary for growth (Fig. 6). The results herein highlight the potential therapeutic benefit of targeting signaling and metabolic pathways that control glucose utilization with pharmacological inhibitors. Indeed, the regulation of glucose metabolism is increasingly recognized to play an important role in tumor formation [28,29]. Aberrant glucose transport and utilization on its own has been implicated in the development and progression of lymphomas [48]. We suggest that anthracycline-based chemotherapy in combination with pharmacological inhibition of PI-3K-linked glucose metabolism may prove beneficial in the treatment of DLBCL.

Acknowledgements

We thank Dr. Raju Chaganti (Memorial Sloan-Kettering Cancer Center, New York, NY) for providing the human OCI LY1 and LY18 cell lines. *Grant Support*: This work was supported by USPHS grant AI-49994 (TCC).

REFERENCES

[1] Moreno JJ. Resveratrol modulates arachidonic acid release, prostaglandin synthesis, and 3T6 fibroblast growth. J Pharmacol Exp Ther 2000;294:333–8.
[2] Subbaramaiah K, Chung WJ, Michaluart P, Telang N, Tanabe T, Inoue H, et al. Resveratrol inhibits cyclooxygenase-2 transcription and activity in phorbol ester-treated human mammary epithelial cells. J Biol Chem 1998;273:21875–82.

[3] Jang M, Cai L, Udeani GO, Slowing KV, Thomas CF, Beecher CW, et al. Cancer chemopreventive activity of resveratrol, a natural product derived from grapes. Science 1997;275:218–20.
[4] Holmes-McNary M, Baldwin AS. Chemopreventive properties of trans-resveratrol are associated with inhibition of activation of the IkappaB kinase. Cancer Res 2000;60:3477–83.
[5] Manna SK, Mukhopadhyay A, Aggarwal BB. Resveratrol suppresses TNF-induced activation of nuclear transcription factors NF-kappa B, activator protein-1, and apoptosis: potential role of reactive oxygen intermediates and lipid peroxidation. J Immunol 2000;164:6509–19.
[6] Fontecave M, Lepoivre M, Elleingand E, Gerez C, Guittet O. Resveratrol, a remarkable inhibitor of ribonucleotide reductase. FEBS Lett 1998;421:277–9.
[7] Sun NJ, Woo SH, Cassady JM, Snapka RM. DNA polymerase and topoisomerase II inhibitors from *Psoralea corylifolia*. J Nat Prod 1998;61:362–6.
[8] She QB, Huang C, Zhang Y, Dong Z. Involvement of c-jun NH_2-terminal kinases in resveratrol-induced activation of p53 and apoptosis. Mol Carcinogenesis 2002;33:244–50.
[9] She QB, Bode AM, Ma WY, Chen NY, Dong Z. Resveratrol-induced activation of p53 and apoptosis is mediated by extracellular-signal-regulated protein kinases and p38 MAPK. Cancer Res 2001;61:1604–10.
[10] Mitchell SH, Zhu W, Young CY. Resveratrol inhibits the expression and function of the androgen receptor in LNCaP prostate cancer cells. Cancer Res 1999;59:5892–5.
[11] Hsieh TC, Wu JM. Differential effects on growth, cell cycle arrest, and induction of apoptosis by resveratrol in human prostate cancer cell lines. Exp Cell Res 1999;249:109–15.
[12] Surh YJ, Hurh YJ, Kang JY, Lee E, Kong G, Lee SJ. Resveratrol, an antioxidant present in red wine, induces apoptosis in human promyelocytic leukemia (HL-60) cells. Cancer Lett 1999;140:1–10.
[13] Dorrie J, Gerauer H, Wachter Y, Zunino SJ. Resveratrol induces extensive apoptosis by depolarizing mitochondrial membranes and activating caspase-9 in acute lymphoblastic leukemia cells. Cancer Res 2001;61:4731–9.
[14] Clement MV, Hirpara JL, Chawdhury SH, Pervaiz S. Chemopreventive agent resveratrol, a natural product derived from grapes, triggers CD95 signaling-dependent apoptosis in human tumor cells. Blood 1998;92:996–1002.
[15] Ansell SM, Armitage J. Non-Hodgkin lymphoma: diagnosis and treatment. Mayo Clin Proc 2005;80:1087–97.
[16] Abramson JS, Shipp MA. Advances in the biology and therapy of diffuse large B-cell lymphoma: moving toward a molecularly targeted approach. Blood 2005;106:1164–74.
[17] Armitage JO, Weisenburger DD. New approach to classifying non-Hodgkin's lymphomas: clinical features of the major histologic subtypes. Non-Hodgkin's Lymphoma Classification Project. J Clin Oncol 1998;16:2780–95.
[18] Alizadeh AA, Eisen MB, Davis RE, Ma C, Lossos IS, Rosenwald A, et al. Distinct types of diffuse large B-cell lymphoma identified by gene expression profiling. Nature 2000;403:503–11.
[19] Shipp MA, Ross KN, Tamayo P, Weng AP, Kutok JL, Aguiar RC, et al. Diffuse large B-cell lymphoma outcome prediction by gene-expression profiling and supervised machine learning. Nat Med 2002;8:68–74.
[20] Davis RE, Brown KD, Siebenlist U, Staudt LM. Constitutive nuclear factor κB activity is required for survival of activated B cell-like diffuse large B cell lymphoma cells. J Exp Med 2001;194:1861–74.
[21] Monti S, Savage KJ, Kutok JL, Feuerhake F, Kurtin P, Mihm M, et al. Molecular profiling of diffuse large B-cell lymphoma identifies robust subtypes including one characterized by host inflammatory response. Blood 2005;105:1851–61.
[22] Rosenwald A, Wright G, Leroy K, Yu X, Gaulard P, Gascoyne RD, et al. Molecular diagnosis of primary mediastinal B cell lymphoma identifies a clinically favorable subgroup of diffuse large B cell lymphoma related to Hodgkin lymphoma. J Exp Med 2003;198:851–62.
[23] Savage KJ, Monti S, Kutok JL, Cattoretti G, Neuberg D, De Leval L, et al. The molecular signature of mediastinal large B-cell lymphoma differs from that of other diffuse large B-cell lymphomas and shares features with classical Hodgkin lymphoma. Blood 2003;102:3871–9.
[24] Downward J. PI 3-kinase, Akt and cell survival. Semin Cell Dev Biol 2004;15:177–82.
[25] Amaravadi R, Thompson CB. The survival kinases Akt and Pim as potential pharmacological targets. J Clin Invest 2005;115:2618–24.
[26] Luo J, Manning BD, Cantley LC. Targeting the PI3K-Akt pathway in human cancer: rationale and promise. Cancer Cell 2003;4:257–62.
[27] Stephens L, Anderson K, Stokoe D, Erdjument-Bromage H, Painter GF, Holmes AB, et al. Protein kinase B kinases that mediate phosphatidylinositol 3,4,5-trisphosphate-dependent activation of protein kinase B. Science 1998;279:710–4.
[28] Plas DR, Thompson CB. Akt-dependent transformation: there is more to growth than just surviving. Oncogene 2005;24:7435–42.
[29] Elstrom RL, Bauer DE, Buzzai M, Karnauskas R, Harris MH, Plas DR, et al. Akt stimulates aerobic glycolysis in cancer cells. Cancer Res 2004;64:3892–9.
[30] Rathmell JC, Fox CJ, Plas DR, Hammerman PS, Cinalli RM, Thompson CB. Akt-directed glucose metabolism can prevent Bax conformation change and promote growth factor-independent survival. Mol Cell Biol 2003;23:7315–28.
[31] Mehra S, Messner H, Minden M, Chaganti RS. Molecular cytogenetic characterization of non-Hodgkin lymphoma cell lines. Genes Chromosomes Cancer 2003;33:225–34.
[32] Doughty CA, Bleiman BF, Wagner DJ, Dufort FJ, Mataraza JM, Roberts MF, et al. Antigen receptor-mediated changes in glucose metabolism in B lymphocytes: role of phosphatidylinositol 3-kinase signaling in the glycolytic control of growth. Blood 2006;107:4458–65.
[33] Frauwirth KA, Riley JL, Harris MH, Parry RV, Rathmell JC, Plas DR, et al. The CD28 signaling pathway regulates glucose metabolism. Immunity 2002;16:769–77.
[34] Ciulla RA, Roberts MF. Effects of osmotic stress on Methanococcus thermolithotrophicus: 13C-edited 1H-NMR studies of osmolyte turnover. Biochim Biophys Acta 1999;1427:193–204.
[35] Yang L, Dan HC, Sun M, Liu Q, Sun XM, Feldman RI, et al. Akt/protein kinase B signaling inhibitor-2, a selective small molecule inhibitor of Akt signaling with antitumor activity in cancer cells overexpressing Akt. Cancer Res 2004;64:4394–9.
[36] Rathmell JC, Vander Heiden MG, Harris MH, Frauwirth KA, Thompson CB. In the absence of extrinsic signals, nutrient utilization by lymphocytes is insufficient to maintain either cell size or viability. Mol Cell 2000;6:683–92.
[37] Shaffer AL, Rosenwald AM, Hurt EM, Giltane JM, Lam LT, Pickeral OK, et al. Signatures of the immune response. Immunity 2001;15:375–85.
[38] Geschwind JF, Georgiades CS, Ko YH, Pedersen PL. Recently elucidated energy catabolism pathways provide opportunities for novel treatments in hepatocellular carcinoma. Exp Rev Anticancer Ther 2004;4:449–57.
[39] Su JL, Lin MT, Hong CC, Chang CC, Shiah SG, Wu CW, et al. Resveratrol induces FasL-related apoptosis through Cdc42

activation of ASK1/JNK-dependent signaling pathway in human leukemia HL-60 cells. Carcinogenesis 2005;26:1–10.
[40] Fukuda R, Hayashi A, Utsunomiya A, Nukuda Y, Fukui R, Itoh K, et al. Alteration of phosphatidylinositol 3-kinase cascade in the multilobulated nuclear formation of adult T cell leukemia/lymphoma (ATLL). Proc Natl Acad Sci USA 2005;102:15213–8.
[41] Tjin EP, Groen RW, Vogelzang I, Derksen PW, Klok MD, Meijer HP, et al. Functional analysis of HGF/MET signaling and aberrant HGF-activator expression in diffuse large B-cell lymphoma. Blood 2006;107:760–8.
[42] Vivanco I, Sawyers CL. The phosphatidylinositol 3-Kinase AKT pathway in human cancer. Nat Rev Cancer 2002;2:489–501.
[43] Speaks SL, Sanger WG, Masih AS, Harrington DS, Hess M, Armitage JO. Recurrent abnormalities of chromosome bands 10q23-25 in non-Hodgkin's lymphoma. Genes Chromosomes Cancer 1992;5:239–43.
[44] Butler MP, Wang SI, Chaganti RS, Parsons R, Dalla-Favera R. Analysis of PTEN mutations and deletions in B-cell non-Hodgkin's lymphomas. Genes Chromosomes Cancer 1999;24:322–7.
[45] Warburg O. On the origin of cancer cells. Science 1956;123:309–14.
[46] Mathupala SP, Rempel A, Pedersen PL. Aberrant glycolytic metabolism of cancer cells: a remarkable coordination of genetic, transcriptional, post-translational, and mutational events that lead to a critical role for type II hexokinase. J Bioenerg Biomembr 1997;29:339–43.
[47] Engel M, Mazurek S, Eigenbrodt E, Welter C. Phosphoglycerate mutase-derived polypeptide inhibits glycolytic flux and induces cell growth arrest in tumor cell lines. J Biol Chem 2004;279:35803–12.
[48] Elstrom R, Guan L, Baker G, Nakhoda K, Vergilio JA, Zhuang H, et al. Utility of FDG-PET scanning in lymphoma by WHO classification. Blood 2003;101:3875–6.